Bistatic MIMO Radar Space-time Adaptive Processing

Jun Li[1,2], Guisheng Liao[1]
[1]National Lab of Radar Signal Processing
Xidian University
Xi'an, China
junli01@mail.xidian.edu.cn

Hugh Griffiths[2]
[2]Department of Electronic and Electrical Engineering
University College London
London, UK
h.griffiths@ee.ucl.ac.uk

***Abstract*—Bistatic multiple-input multiple-output (MIMO) radar systems have the advantages of both bistatic radar and MIMO radar. In addition, the transmit angle can be obtained by processing the receive data. In this paper, bistatic MIMO and space-time adaptive processing (STAP) are applied to ground moving target indication (GMTI). It is shown that the clutter spectrum is a curve in 3-dimensions (transmit angle, receive angle and Doppler frequency) after compensation. The performances of single input multiple-output (SIMO) and MIMO cases are compared. The results show that the bistatic MIMO-STAP outperforms its SIMO counterparts in both signal interference and noise ratio (SINR) and SINR loss.**

I. INTRODUCTION

Multiple-input multiple-output (MIMO) radar is a relatively new term for a radar field which has been inspired by the MIMO technique in communications. As shown in Figure 1, MIMO radar has multiple transmit channels and multiple receive channels, and the transmit channels can be separated by waveforms, or time, or frequencies, or polarizations at each receiver. So the number of channels of a MIMO radar is increased substantially compared to its single input single-output (SIMO) counterparts. Most of the advantages of the MIMO radar come from increasing the number of channels. Two main classes of MIMO radar have been proposed: with widely separated antennas [1] and with co-located antennas [2]. The first class utilizes the diverse scattering properties of a target from sufficiently spaced antennas to improve the performance of the systems. The second class allows the improvement of the radar performances by coherent processing the multiple channels. In fact, the information of transmit channels, such as loss coefficients or transmit angles are also obtained when the transmit channels are separated at the receivers.

In [3], the MIMO technique has been extended to space-time adaptive processing (STAP). It was shown that the signal-to-interference and noise ratio (SINR) performance of MIMO-STAP radar is better than the corresponding SIMO one. [4] considers the clutter rank of MIMO-STAP and indicated that the ratio of clutter rank and the total dimension of space steering vector of MIMO radar is smaller than for SIMO. So MIMO radar receiver can null out the clutter subspace with little effect on SINR.

A scheme of bistatic MIMO radar has recently been proposed for target localization [5]. Bistatic MIMO radar has the potential advantages both of bistatic radar, such as reduced space loss, covert operation, and reduced susceptibility to jamming [6], and of MIMO radar, such as additional spatial degrees of freedom (DoFs) [2]. Also, bistatic MIMO radar has the particular advantage of being able to obtain the transmit angle information (direction of departure) by processing the received data. Several publications have studied direction of departure and direction of arrival estimation for bistatic MIMO radar [7-9]. In this paper, we extend the usage of bistatic MIMO radar to ground moving target indicator (GMTI). Space-time adaptive processing is applied to bistatic MIMO radar to cancel the clutter. It is shown that clutter spectrum is a curve in 3-dimension space of transmit angle, receive angle and Doppler frequency other than traditional 2-dimension clutter spectrum. The performances of SIMO and MIMO bistatic radar are compared in this paper.

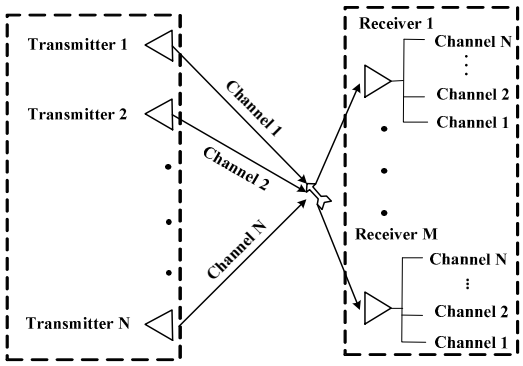

Figure 1. MIMO radar structure

II. BISTATIC MIMO-STAP RADAR CONFIGURATION AND CLUTTER MODEL

Figure 2 shows the geometry of the bistatic MIMO radar. We take the location of the receiver *O* as the origin of the coordinate system. The *x*-axis points in the same direction as

Supported by the National Science Fund for Distinguished Young Scholars (No.60825104) and Program for Changjiang Scholars and Innovative Research Team in University (IRT 0954)

the velocity vector of receiver and the coordinates of the receiver are $[0,0,z_r]$. The X-Y plane is on the ground plane and Z -axis points vertically upwards. o is the location of the transmitter and the length of the baseline Oo is L_b. All the angles in the X-Y plane are measured with respect to the X-axis. γ is the elevation of the transmitter. ϕ_v is the direction of the velocity vector of the transmitter. ϕ_r and ϕ_t are the directions of array axis of receiver and transmitter respectively. $\theta_{r,i}$ and $\theta_{t,i}$ are the receiver and transmitter azimuth of the i th clutter patch of a given range cell. $\varphi_{r,i}$ and $\varphi_{t,i}$ are the corresponding elevations of that clutter patch. The α_i and β_i are the cone angles of the i th clutter patch in one range cell with respect to receiver and transmitter axes respectively. The locus of ground clutter scatters at a given bistatic range is an ellipse.

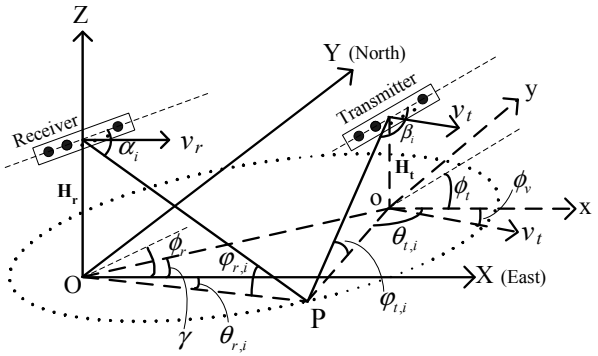

Figure 2. Bistatic radar geometry

The transmit and receive arrays are assumed to be uniform linear arrays (ULAs) with M elements at the transmitter and N elements at the receiver. The elements at the transmitter and receiver are omnidirectional. d_t is the inter-element spacing at the transmitter and d_r is the inter-element spacing at the receiver. λ denotes the carrier wavelength. Assume there are L pulses in a coherent processing interval (CPI) with pulse repetition interval (PRI) T. We first define the normalized receive spatial frequency, transmit spatial frequency and Doppler frequency at the i th clutter patch as follows:

$$f_{sr,i} = \frac{d_r}{\lambda}\cos(\phi_r - \theta_{r,i})\cos\varphi_{r,i} = \frac{d_r}{\lambda}\cos\alpha_i \tag{1}$$

$$f_{st,i} = \frac{d_t}{\lambda}\cos(\phi_t - \theta_{t,i})\cos\varphi_{t,i} = \frac{d_t}{\lambda}\cos\beta_i \tag{2}$$

$$f_{d,i} = \frac{v_r T}{\lambda}\cos(\theta_{r,i})\cos\varphi_{r,i} + \frac{v_t T}{\lambda}\cos(\phi_v - \theta_{t,i})\cos\varphi_{t,i} \tag{3}$$

The received clutter of the given range cell of the n th element at the l th pulse can be expressed as follows:

$$y_{n,l} = \sum_{i=0}^{N_c-1}\sum_{m=0}^{M-1}\rho_i s_m(\tau)e^{j2\pi[f_{st,i}m + f_{sr,i}n + f_{d,i}l)]} \tag{4}$$

where ρ_i is the signal reflected coefficient by the i th clutter patch. s_m is the waveform from the m th transmitting element and N_c is the number of clutter patches in one range cell.

The sufficient statistics can be extracted by a bank of matched filters. The result of the clutter sufficient statistics is as follows:

$$y_{n,m,l} = \sum_{i=0}^{N_c-1}\rho_i e^{j2\pi n f_{sr,i}}e^{j2\pi f_{st,i}}e^{j2\pi f_{d,i}l} \tag{5}$$

Here we assume that the transmitting waveforms $s_m(\tau)$ are orthogonal to each other, that is

$$\int s_m(\tau)s_k^*(\tau)d\tau = \delta_{mk} \tag{6}$$

The clutter model corresponding to one range cell can be written as the $MNL\times 1$ vector:

$$\mathbf{y}_c = \sum_{i=1}^{N_c}\rho_i \mathbf{g}(f_{sr,i}, f_{st,i}, f_{d,i}) \tag{7}$$

where $\mathbf{g}(f_{sr,i}, f_{st,i}, f_{d,i}) = \mathbf{a}(f_{sr,i})\otimes\mathbf{b}(f_{st,i})\otimes\mathbf{c}(f_{d,i})$ and $\otimes$ denotes the Kronecker product.

$$\mathbf{a}(f_{sr,i}) = [1, e^{j2\pi f_{sr,i}}, \cdots, e^{j2\pi(N-1)f_{st,i}}]$$

$$\mathbf{b}(f_{st,i}) = [1, e^{j2\pi f_{st,i}}, \cdots, e^{j2\pi(M-1)f_{st,i}}]$$

$$\mathbf{c}(f_{d,i}) = [1, e^{j2\pi f_{d,i}}, \cdots, e^{j2\pi(L-1)f_{d,i}}]$$

III. 3-D CLUTTER SPECTRUM AND CANCELLATION

In this section, we will show the 3-D clutter spectrum of bistatic MIMO-STAP radar in various cases. All the numerical examples in this paper are based on the parameters listed in Table I.

TABLE I. PARAMETERS FOR BISTATIC RADAR OPERATION

Number of transmitting elements	M	5
Number of receiving elements	N	10
number of coherence pulses	L	10
Carrier Frequency		1.24 GHz
Pulse Repetition Frequency		2000 Hz
Baseline length	L_b	100 km
Receiver height	H_r	5000 m
Receiver velocity	v_r	100 m/s
Receiver flight direction		0^0 , with respect to x-axis
Transmitter elevation	γ	135^0
Transmitter height	H_t	10000 m
Transmitter velocity	v_t	100 m/s, 0 (stationary)
Transmitter flight direction	ϕ_v	90^0 with respect to x-axis

A. Side-looking

In this case, we assume that the transmitter and the receiver velocities are consistent with their array axes respectively, that is $\phi_r = 0$ and $\phi_t = \phi_v$. Substituting (1), (2) into (3), we can obtain the equation as follows

$$f_{d,i} = \frac{v_r T}{d_r}f_{sr,i} + \frac{v_t T}{d_t}f_{st,i} \tag{8}$$

From (8), it is clear that Doppler frequency is a function of transmit spatial frequency and receive spatial frequency. The transmit angle and the receive angle are restricted by the iso-range ellipse. So the clutter spectrum will be a curve in 3-dimensions of transmit angle, receive angle and Doppler frequency. Furthermore, all the clutter scatterers will be within a plane, as (8) is the equation of a plane in 3-dimensional space with parameters $[f_{d,i}, f_{sr,i}, f_{st,i}]$.

Figure 3 shows the 3-D clutter spectrum curves of bistatic MIMO-STAP radar in the side-looking case. From Figure 3 (a), it can be observed that the clutter spectra are range-dependence in a 3-D plane. In Figure 3 (b) and (c), the clutter spectra are projected to transmit-Doppler and receive-Doppler planes respectively. It's shown that the clutter spectra are also range-dependence. To get the range-independence clutter, the f_{sr} and f_{st} axes are rotated an angle ψ with respect to Doppler axis f_d, and then the clutter spectra are projected on this new coordination system. The result is plotted in Figure 3(d). By using (8), the angle ψ can be calculated as follows

$$\psi = \mathrm{a}\tan(\frac{v_t}{v_r}) \tag{9}$$

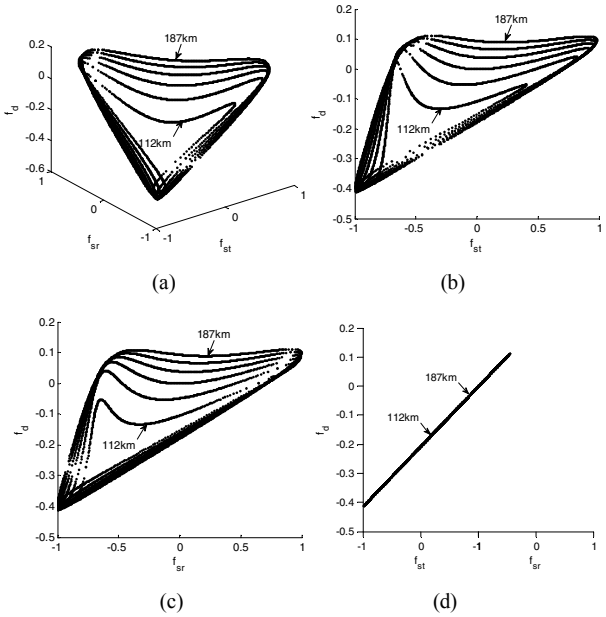

Figure 3. 3-D clutter spectrum curve of bistatic MIMO-STAP radar in the side-looking case. (a) 3-D clutter spectrum. (b) projection on Transmit-Doppler plane. (c) projection on Receive-Doppler plane. (d) projection after rotating in Transmit-Receive angle plane

B. Stationary transmitter

In this case, we assume the transmitter is stationary, that is $v_t = 0$. Then (8) can be written as

$$f_{d,i} = \frac{v_r T}{d_r} f_{sr,i} \tag{10}$$

This means that the Doppler is coupled with receive angle. From Figure 4(b), it is seen that clutter spectra are range-independent in the Doppler-receive angle plane. But the DoFs from transmitter are lost. This is just equal to the corresponding SIMO radar whose transmit weights are all 1. It is interesting that these virtual transmit weights can be changed in the receiver, as the real transmitter is omnidirectional. It implies the ability of MIMO radar for forming the virtual transmit beam in receiver. To exploit the DoFs from the transmitter, range-dependence in Figure 4(a) should be compensated by the data processing.

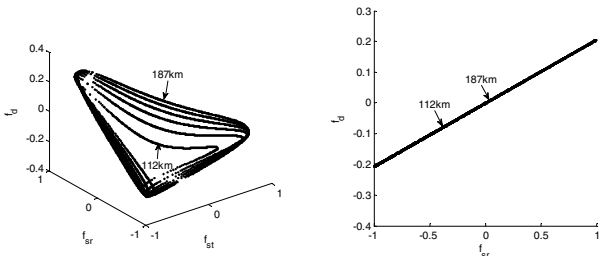

Figure 4. 3-D clutter spectrum curve of bistatic MIMO-STAP radar in the stationary transmitter case. (a) 3-D clutter spectra. (b) projection on doppler-receive angle plane.

C. Non-side-looking

In the case of non-side-looking bistatic MIMO radar, the clutter spectra are no longer a plane in 3-D. The range-dependence clutter spectra cannot transform to range-independence by projection. In Figure 5, the clutter spectra are plotted for $\phi_r = \frac{\pi}{6}$.

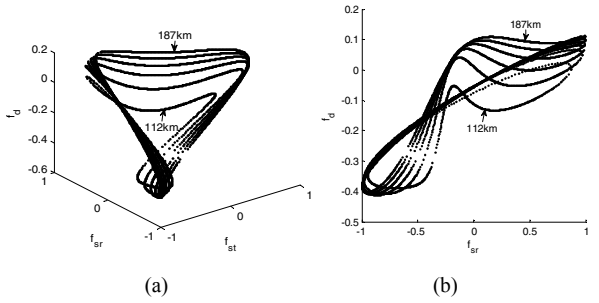

Figure 5. 3-D clutter spectrum curve of bistatic MIMO-STAP radar ($\phi_r = \frac{\pi}{6}$). (a) 3-D clutter spectrum. (b) projection on Receive-Doppler plane

D. Clutter cancellation

To cancel the clutter, the clutter covariance matrix (CCM) $\mathbf{R}_c$ should be estimated. The maximum-likelihood (ML) estimate can be achieved by averaging of neighboring data snapshots when the clutter data are independent and identically distributed (iid) with respect to range [10]. However, we can see from above that the 3-D clutter data are not iid with respect range for bistatic MIMO-STAP radar. In the cases A and B, the range-dependence can be transformed to range-independence by projection. But the DoFs from the

transmitter will be lost. The range-dependence compensation should be performed to obtain the performance gain of MIMO radar.

Since the range-dependence is visible in the 3-D spectral domain as shown in Figure 3-5, we can perform the range-dependence compensation in this domain directly. The idea is to bring the clutter ridge of each range into registration with that of reference range. This idea has been used in 2-D clutter range-dependence compensation in [11] called "registration-based compensation" (RBC). The 3-D RBC method will be described in detail in another paper. In this paper, we focus on the evaluation of the performances of bistatic MIMO-STAP radar. So we just use the result after compensation.

STAP linearly combines the elements of received snapshot to maximize the SINR. The adaptive weight vector for a particular angle and Doppler patch of interest is [10]

$$\mathbf{w}_k = \mu \mathbf{R}_k^{-1} \mathbf{g}(f_{sr,i}, f_{st,i}, f_{d,i}) \tag{11}$$

where μ is a scalar and $\mathbf{R}_k$ is the k th range cell data covariance matrix calculated by compensated snapshots with noise.

IV. PERFORMANCE EVALUATION

The performances of bistatic MIMO-STAP radar are evaluated by simulations in this section. We compare it with its SIMO counterparts in the case of same geometry and same hardware configuration. For MIMO radar, each transmitting element transmits unit power waveform and the waveforms of the different elements are orthogonal to each other. For the SIMO case, all the transmitting elements transmit the same waveform with different phase, so the beam can be formed at certain spatial area. Therefore, SIMO radar enjoys the beam gain compared to MIMO radar for particular angle of interest. However, the SIMO radar systems have to transmit several directional beams in order to scan a given region of interest (ROI) whereas MIMO radar systems transmit omnidirectional. Instead of M directional beams, one omnidirectional beam can be transmitted with M times higher time-on-target (TOT) interval [3,12]. The TOT compensation will be considered in the following simulations.

The radar system is side-looking for both transmitter and receiver. The transmitting and receiving spatial frequencies of interested cell are $f_{sr,i} = 0.1037$ and $f_{st,i} = 0$ respectively. The noise power of each receive element is assumed as 0.1. Other parameters are listed in Table I. 3-D clutter cancellation by STAP is applied to bistatic MIMO radar systems. SINR and SINR loss by using SIMO and MIMO radar systems are plotted in Figure 6. It is shown that the performance of bistatic MIMO-STAP radar outperform the bistatic SIMO-STAP radar in both SINR and SINR loss. It can be observed that the MIMO cases have high output SINR, so they can achieve better target detection performance. Also, we can observe from the notch that the minimum detectable velocity (MDV) of MIMO case is better than that of SIMO one. Furthermore, there is only one notch in SINR and SINR loss for the MIMO case, whereas the SIMO case has two notches. The reason is that the clutter is cancelled in 3-D and the Doppler ambiguity is avoided in the case of MIMO.

V. CONCLUSION

Bistatic MIMO-STAP scheme has been proposed in this paper. The clutter spectrum in this scheme is a curve in 3-D space composed of transmit angle, receive angle and Doppler frequency. The clutter can be cancelled after the range-dependence compensation. It has been shown that the performance of bistatic MIMO-STAP radar is better than bistatic SIMO-STAP radar. Furthermore, there is only one notch for SINR and SINR loss for bistatic MIMO-STAP radar in the case of omnidirectional transmit and receive elements.

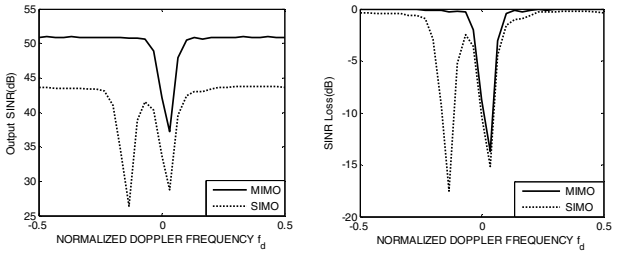

(a) (b)

Figure 6. Comparison of MIMO and SIMO STAP radar. (a) comparison of SINR. (b) comparison of SINR loss.

REFERENCES

[1] A. Haimovich, R. Blum and L. Cimini, "MIMO radar with widely separated antennas," *IEEE Signal Processing Magazine*, vol. 25, Jan. 2008, pp. 116–129.

[2] Jian Li and P. Stoica, "MIMO radar with colocated antennas," *IEEE Signal Processing Magazine*, vol. 24, Sept. 2007, pp. 106–114.

[3] D. W. Bliss and K. W. Forsythe, "Multiple-input multiple-output (MIMO) radar and imaging: degrees of freedom and resolution," *in Proc. 37th IEEE Asilomar Conf. on Signals, Systems, and Computers,* vol. 1, pp. 54–59, Nov. 2003.

[4] Chun-Yang Chen and P. P. Vaidyanathan: "MIMO radar space-time adaptive processing using prolate spheroidal wave function," *IEEE Trans. Signal Processing*, 2008, 56, (2), pp.623-635.

[5] Haidong Yan, Jun Li and Guisheng Liao, "Multitarget identification and localization using bistatic MIMO radar systems," *EURASIP Journal on Advances in Signal Processing*, vol. 2008, Article ID 283483, 8 pages, 2008.

[6] N. J. Willis and H. D. Griffiths, *Advances in Bistatic Radar*, SciTech Publishing, Raleigh, NC, 2007.

[7] Ming Jin, Guisheng Liao and Jun Li, "Joint DOD and DOA estimation for bistatic MIMO radar," *Signal Processing*, vol. 89, no. 2, February 2009, pp. 244-251

[8] Nion D. and Sidiropoulos N.D., "A PARAFAC-based technique for detection and localization of multiple targets in a MIMO radar system," *Proc. IEEE International Conference on Acoustics, Speech and Signal Processing*, pp. 2077–2080, 19-24 April 2009.

[9] Jun Li, Guisheng Liao, Kejiang Ma and Cao Zeng. "Waveform decorrelation for multitarget localization in bistatic MIMO radar systems," *in Proc. 2010 IEEE International Radar Conference*, Washington, May 2010.

[10] I.S. Reed, J.D. Mallet and L.E. Brennan, "Rapid convergence rate in adaptive arrays," *IEEE Trans. AES*, vol.10, no.6, pp.853-863, Nov. 1974.

[11] F.D. Lapierre, M. Van Droogenbroeck, and J.G. Verly, "New solutions to the problem of range dependence in bistatic STAP radar," *Proc. IEEE Radar Conference*, Huntsville, AL, 5-8 May 2003.

[12] I. Bekkerman and J. Tabrikian, "Target detection and localization using MIMO radars and sonars," *IEEE Trans. Signal Processing*, vol. 54, no. 10, pp. 3873–3883, 2006.